GMR
The Original

# BIOGENIC SYNTHESIS OF CuO NANOPARTICLES LOADED WITH POLYMERIC NANOSCAFFOLDS FROM *Padina tetrastromatica* EXTRACT: A STRUCTURAL INSIGHT INTO ANTICANCER ACTIVITY ON HT-29 AND MCF-7 CELLS

**Vishal Suraj Ravindran[1], Manodhar Naidu Vunnam[2], Ramganesh Selvarajan[3]***

[1]Saveetha Medical College & Hospital (SMCH), Saveetha Institute of Medical and Technical Sciences (SIMATS), Thandalam, Chennai, Tamil Nadu 602105, India. klssvishal@gmail.com
[2]Department of Nephrology, Saveetha Medical College and Hospital, Saveetha Institute of Medical And Technical Sciences (SIMATS), Thandalam, Chennai-602105, Tamil Nadu, India. Email: manodharnaidu9@gmail.com
[3]Centre for Microbial Ecology and Translational Research, Department of Microbiology, Saveetha Medical College and Hospital, Saveetha Institute of Medical And Technical Sciences (SIMATS), Thandalam, Chennai-602105, Tamil Nadu, India.
Email: ramganesh.presidency@gmail.com
*Corresponding Author: ramganesh.presidency@gmail.com (R.S.)

**ABSTRACT**
This study developed starch/PVA electrospun nanoscaffolds incorporating *Padina tetrastromatica*-synthesized CuO nanoparticles (NPs) and evaluated their physicochemical and anticancer properties. UV-Vis, Fourier-transform infrared spectroscopy (FTIR), and X-ray diffraction (XRD) confirmed CuO NP formation (monoclinic phase) and scaffold integration, while Scanning electron microscopy (SEM) revealed a porous, fibrous structure. Thermogravimetric analysis (TGA) indicated stability up to 300°C, and Dynamic light scattering (DLS) showed NPs with 108 nm size and -22.13 mV zeta potential. *In vitro* MTT assays against HT-29 and MCF-7 cells demonstrated concentration-dependent cytotoxicity, with nanoscaffolds exhibiting the highest potency ($IC_{50}$: 10–15 µg/mL) compared to CuO NPs (15–25 µg/mL) and algal extract (30–45 µg/mL). The nanoscaffolds' enhanced efficacy is attributed to synergistic effects of CuO NPs and the polymeric matrix, facilitating efficient drug delivery. These results underscore the potential of green-synthesized nanoscaffolds as a biocompatible and effective platform for anticancer therapy.

**KEYWORDS:** *Padina tetrastromatica*, Green synthesis, CuO NPs, Starch/PVA/CuO-NPs nanoscaffolds, Anticancer activity.

## 1. INTRODUCTION

In recent years, the intersection of nanotechnology and biomedicine has ushered in a new era of innovative materials designed to improve cancer diagnosis and treatment [1]. Among the diverse nanomaterials explored, copper oxide nanoparticles (CuO NPs) have garnered considerable attention due to their unique physicochemical properties, biocompatibility, and potent bioactivities, including antimicrobial, antioxidant, and anticancer effects [2]. Their multifaceted functionality makes CuO NPs promising candidates for cancer therapeutics, particularly as drug delivery agents or as components of advanced scaffold systems that support tissue regeneration while exerting cytotoxic effects on tumor cells [3].

Despite their potential, traditional chemical synthesis methods for CuO NPs often involve hazardous reagents and generate toxic by-products, raising environmental and safety concerns [2]. To overcome these limitations, green synthesis approaches have emerged as sustainable alternatives, utilizing biological resources such as plant extracts, microorganisms, and marine algae to reduce metal ions into nanoparticles under mild conditions [4]. This bioinspired synthesis not only minimizes ecological footprints but also imparts intrinsic bioactive molecules onto the nanoparticle surface, enhancing stability and biological efficacy [5].

Among the rich sources of natural bioactives, marine macroalgae have attracted significant interest for nanoparticle synthesis due to their abundant phytochemicals, including polyphenols, polysaccharides, proteins, and pigments, which act as reducing and capping agents [6]. Brown macroalgae, in particular, contain fucoidans, alginates, and other compounds with well-documented antioxidant and anticancer properties [7]. *Padina tetrastromatica,* a widely distributed brown alga found along the Indian coastline, has been shown to possess diverse bioactivities, making it an ideal candidate for green synthesis of CuO NPs [8]. Utilizing ultrasonic-assisted extraction (UAE) methods further enhances the yield and activity of algal bioactives by efficiently disrupting cell walls, leading to enriched extracts that can facilitate nanoparticle formation [9].

While nanoparticles possess impressive individual capabilities, their integration into polymeric nanofibrous scaffolds combines the advantages of nanotechnology and biomaterials science [10]. Electrospinning technology allows the fabrication of continuous nanofibers with high surface area-to-volume ratios, tunable porosity, and

structural resemblance to native extracellular matrix (ECM) [11]. These features are critical for applications in tissue engineering and localized cancer therapy, where scaffolds can act as platforms for controlled drug release and cell interaction [12].

Polyvinyl alcohol (PVA) is a synthetic, biocompatible polymer extensively used in electrospinning due to its hydrophilicity, mechanical strength, and film-forming ability [13]. However, its inherent limitations in biological functionality necessitate blending with natural polymers. Starch, a biodegradable polysaccharide abundant in nature, complements PVA by enhancing scaffold biocompatibility and biodegradability [14]. Incorporating starch within PVA matrices improves mechanical properties and provides sites for nanoparticle binding, which is essential for developing stable nanocomposites [15].

Combining CuO NPs biosynthesized using *P. tetrastromatica* extract with starch/PVA nanofibers presents a promising strategy for creating multifunctional scaffolds with enhanced anticancer efficacy and favorable physicochemical characteristics [16]. The CuO NPs embedded within the nanofibers can exert localized cytotoxic effects on cancer cells, while the biocompatible polymer matrix supports cellular interactions and maintains scaffold integrity [17]. Such hybrid scaffolds are especially attractive for cancer treatment modalities requiring minimal systemic toxicity and targeted therapeutic action [18].

However, to realize the full potential of these composite nanofibrous scaffolds, comprehensive characterization is necessary [19]. Physicochemical analyses such as UV-Visible spectroscopy, Fourier-transform infrared (FTIR) spectroscopy, X-ray diffraction (XRD), scanning electron microscopy (SEM), and thermogravimetric analysis (TGA) provide insights into nanoparticle formation, polymer-nanoparticle interactions, crystallinity, morphology, and thermal stability [20]. Additionally, dynamic light scattering (DLS) and zeta potential measurements elucidate nanoparticle size distribution and colloidal stability, critical factors influencing biological behavior [21].

*In vitro* anticancer activity evaluation using well-established human cancer cell lines, such as HT-29 (colon adenocarcinoma) and MCF-7 (breast cancer), offers preliminary yet vital data on the cytotoxic potential and dose-dependent effects of the scaffolds compared to free nanoparticles and algal extracts alone [22]. MTT assays facilitate quantification of cell viability and proliferation, helping to assess therapeutic efficacy and potential selectivity [23].

The present study aims to harness the green synthesis capabilities of ultrasonic-assisted *P. tetrastromatica* extracts for producing CuO NPs and incorporate them into starch/PVA electrospun nanofibers to fabricate novel bioactive scaffolds [24]. These scaffolds are meticulously designed and characterized for their physicochemical properties and evaluated for anticancer activity against human cancer cell lines [25]. This multidisciplinary approach bridges marine biotechnology, nanomaterials engineering, and cancer biology to develop environmentally friendly, effective nanoscaffolds with translational potential in cancer therapy [26].

By integrating renewable marine resources, green chemistry, and advanced nanofabrication techniques, this research contributes to the expanding field of sustainable nanomedicine [27]. The findings not only enhance understanding of the interactions between biogenic CuO nanoparticles and polymer matrices but also pave the way for future development of multifunctional biomaterials tailored for oncology applications. The novel nanoscaffolds reported here hold promise for improving localized cancer treatment, reducing side effects, and advancing the design of smart therapeutic platforms.

## 2. MATERIALS AND METHODS

### 2.1. Materials

The brown marine macroalga *P. tetrastromatica* was collected from the coastal region of Rameswaram, Tamil Nadu, India, for use in the green synthesis of CuO NPs. Copper(II) sulfate pentahydrate ($CuSO_4 \cdot 5H_2O$; Sigma-Aldrich) was utilized as the metal salt precursor. PVA with an approximate molecular weight of 115,000 was selected as the primary polymer matrix for electrospinning, and native starch sourced locally was added to enhance the scaffold's mechanical properties. All reagents, including ethanol and Milli-Q water (Merck, Sigma-Aldrich), were of analytical grade. Nanofiber fabrication was performed using a HOLMARC HO-NFES-040 electrospinning setup coupled with a precision syringe pump. Characterization techniques employed included UV-Vis spectrophotometry (VIS SPEC V-730), FTIR(PerkinElmer Spectrum Two), XRD (Bruker D8 Advance), SEM (JEOL JSM-IT800 NANO), DLS and zeta potential analysis (Malvern Zetasizer Ultra), and TGA (PerkinElmer TGA 8000). HT-29 and MCF-7 cells were obtained from the National Centre for Cell Science (NCCS), Pune, India, which provided authenticated and contamination-free cell stocks for biological investigations focused on anticancer activity.

### 2.2. Marine macroalgae collection

Samples of *P. tetrastromatica* were handpicked from intertidal zones along the Rameswaram coastline. The collected *Padina tetrastromatica* was taxonomically identified and authenticated by Dr V. Veeragurunathan, CSIR-CSMCRI-Marine Algal Research Station, Mandapam Camp 623519, Tamil Nadu, India. A voucher specimen was prepared and deposited at the Herbarium of the CSIR-CSMCRI-Marine Algal Research Station, under the accession number: SI–2025–RMM–015. This authentication ensures botanical accuracy and standardization of the study material. The collected biomass was initially rinsed under tap water to remove sand, epiphytes, and debris, followed by several thorough washes with distilled water to eliminate residual salt and contaminants. Approximately 100 grams of the cleaned seaweed were cut into smaller portions to facilitate even

drying. These were then air-dried for about two weeks in a shaded, well-ventilated environment to maintain the integrity of bioactive compounds. Once completely dried, the material was pulverized into a uniform fine powder using an electric grinder to standardize particle size for extraction purposes.

### 2.3. Ultrasound-Assisted Extraction (UAE)

For bioactive compound extraction, 2 g of powdered *P. tetrastromatica* was dispersed in 50 mL of Milli-Q water. The mixture underwent ultrasonication in a LABQUEST ultrasonic bath (Borosil; Serial No. 941032329018) at 60°C for 45 minutes. Cavitation effects from the ultrasound facilitated cell wall disruption, enhancing intracellular compound release. Post-sonication, the extract was cooled to room temperature and filtered through sterile Whatman No. 1 filter paper. The filtrate was stored at 10°C for immediate use, while an aliquot was freeze-dried and sealed for long-term storage [28, 29].

### 2.4. Biosynthesis of CuO NPs

CuO NPs were biosynthesized through a green route using the algal extract as both the reducing and capping agent. Ten milligrams of freeze-dried *P. tetrastromatica* extract was dissolved in 10 mL of Milli-Q water and combined with 50 mL of 0.1 M $CuSO_4 \cdot 5H_2O$ in a 5:1 volume ratio. This mixture was magnetically stirred at 650 rpm and maintained at 60°C for 2 hours. The reaction progress was indicated by a color change from blue to a bluish-green hue, signaling the reduction of $Cu^{2+}$ ions. The precipitated CuO NPs were collected by centrifugation, washed thrice with distilled water to remove impurities, and lyophilized for 48 hours. The dried nanopowder was preserved in desiccators for further application [30].

### 2.5. Electrospinning of CuO-starch/PVA nanofibers

Composite nanofibrous mats embedded with CuO NPs were prepared via electrospinning. A 15% (w/w) aqueous PVA solution was first prepared with constant stirring until completely dissolved. Subsequently, 100 mg each of starch and CuO NPs were added to the solution. The blend was heated to 50°C and stirred continuously for 2.5 hours to ensure uniform nanoparticle distribution. The final homogenous solution was transferred into a syringe fitted with a stainless steel needle (0.84 mm inner diameter) and placed in a HOLMARC HO-NFES-040 electrospinning machine. Electrospinning was conducted at room temperature under optimized parameters: 11.5 kV applied voltage, 12.3 cm distance between the needle and collector, and a flow rate of 0.4 mL/h. The process lasted between 6 and 8 hours, resulting in nanofiber mats that were peeled from aluminum foil and stored in a desiccator [31-33].

### 2.6. Characterization of nanoparticles and nanofiber scaffolds

#### 2.6.1. UV-visible spectroscopy

UV-Vis absorption spectra of synthesized CuO NPs were recorded using a VIS SPEC V-730 spectrophotometer over the wavelength range of 200 to 800 nm, with deionized water as the reference blank. Characteristic absorbance peaks, attributed to surface plasmon resonance, confirmed nanoparticle synthesis [34].

#### 2.6.2. FTIR spectroscopy analysis

FTIR spectra for the CuO NPs and composite nanofibers were acquired using a PerkinElmer Spectrum Two FTIR spectrometer equipped with an ATR accessory. Scanning was performed over 4000 to 400 $cm^{-1}$ at a spectral resolution of 4 $cm^{-1}$, averaging 64 scans per sample. Spectra displayed functional groups such as hydroxyl, phenolic, carboxylate, and Cu–O bond vibrations, indicating successful integration of the bioactive components and nanoparticles in the scaffold [35].

#### 2.6.3. XRD analysis

The crystallinity and phase purity of CuO NPs and composite scaffolds were evaluated with a Bruker D8 Advance X-ray diffractometer utilizing CuKα radiation (λ = 1.5406 Å). Scans were conducted from 5° to 90° 2θ with a step size of 0.029649°, under 40 kV and 40 mA settings. Diffractogram peaks were matched with standard JCPDS files to verify CuO formation and incorporation [8].

#### 2.6.4. SEM analysis

Surface morphology and nanoparticle distribution within the nanofibers were examined via a JEOL JSM-IT800 NANO SEM. Samples were sputter-coated with gold to enhance electrical conductivity before imaging. SEM micrographs revealed uniform fibers with well-embedded nanoparticles and a porous microstructure, confirming scaffold integrity [36].

#### 2.6.5. TGA

Thermal stability and compositional changes were assessed using PerkinElmer TGA 8000. Approximately 5 mg of each sample was heated from room temperature to 550°C at a rate of 15°C/min under nitrogen flow. Weight loss patterns corresponded to moisture evaporation, polymer degradation, and residue formation, providing insights into scaffold thermal behavior [37].

#### 2.6.6. Particle size and zeta potential

DLS and zeta potential analyses were performed using a Malvern Zetasizer Ultra to measure nanoparticle size distribution and surface charge, respectively. High absolute zeta potential values suggested good colloidal stability by preventing particle agglomeration in aqueous dispersion [38].

All raw and processed data are accessible in the Mendeley Data repository via DOI:10.17632/ddbgcpm32x.2.

### 2.7. *In Vitro* anticancer activity

#### 2.7.1. Cell lines and culture conditions

Human colon adenocarcinoma (HT-29) and breast cancer (MCF-7) cell lines were procured from the National Center for Cell Science (NCCS), Pune, India. Cells were cultured in Minimum Essential Medium (MEM) supplemented with 10% fetal bovine serum (FBS) and maintained at 37°C with 5% $CO_2$ atmosphere [39].

#### 2.7.2. MTT assay for cell viability

HT-29 and MCF-7 cells were seeded in 96-well plates at a density of $5 \times 10^5$ cells per well and incubated overnight for adherence. Cells were treated with varying concentrations (6.25, 12.5, 25, 50, and 100 µg/mL) of algal extract, CuO NPs, and starch/PVA/CuO nanoparticle nanoscaffolds, in triplicates, followed by incubation for 24 hours at 37°C and 5% $CO_2$. Subsequently, MTT reagent was added to each well and incubated for 4 hours. The resultant formazan crystals were solubilized in 200 µL of dimethyl sulfoxide (DMSO), and absorbance was recorded at 570 nm using a spectrophotometer. Experiments were performed in triplicate independently, and mean values with standard deviations were calculated [40].

### 2.8. Statistical analysis

Statistical evaluations were carried out using SPSS v25.0 and GraphPad Prism 9.0 software. Experimental results from triplicate trials are expressed as mean ± standard deviation. Group differences were assessed by one-way ANOVA followed by post-hoc tests such as Tukey's or Dunnett's where appropriate. Statistical significance was set at $p < 0.05$. Pearson correlation coefficients were calculated to analyze variable relationships. Data normality was tested using the Shapiro–Wilk method; datasets failing normality were logarithmically transformed before analysis. A 95% confidence interval was applied for all statistical interpretations [41].

## 3. RESULTS

### 3.1. UV-visible spectroscopy

The UV-Vis spectra (Fig. 1) of *P. tetrastromatica* extract and the synthesized CuO NPs were recorded using a JASCO V-730 spectrophotometer within the 200–800 nm wavelength range, capturing data points every 1 nm with a bandwidth of 1.0 nm. The CuO NPs displayed a distinct absorption peak at 273 nm (absorbance: 0.547), attributed to surface plasmon resonance (SPR), confirming nanoparticle formation. In contrast, the algal extract did not show a notable absorption peak, revealing distinct optical properties. Measurements were acquired at a scan rate of 1000 nm/min with baseline correction applied to enhance precision. This spectral evaluation highlights the utility of UV-Vis spectroscopy in verifying nanoparticle synthesis and differentiating the optical profiles of biological extracts.

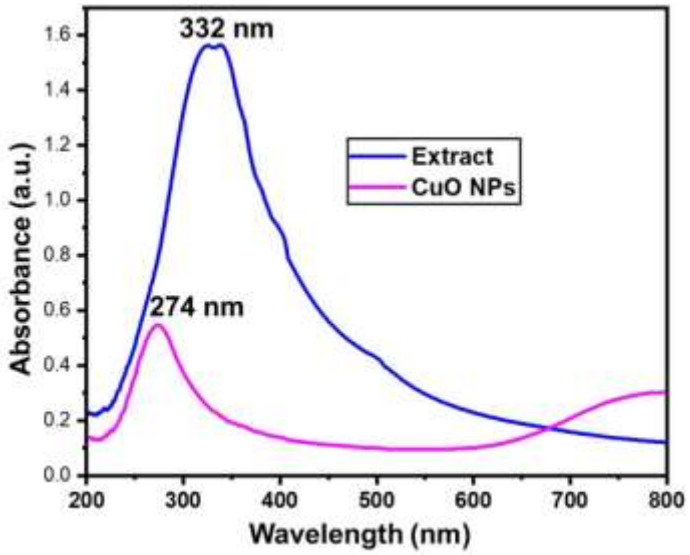


**Fig. 1. UV–Visible spectral profiles of algal extract and CuO NPs.**

### 3.2. FTIR spectroscopy analysis

FTIR spectra (Fig. 2), acquired on a PerkinElmer Spectrum IR instrument over the range of 4000–400 $cm^{-1}$, were used to characterize chemical functional groups present in CuO NPs and starch/PVA nanoscaffolds. The CuO NPs exhibited characteristic absorption bands at 602.84 $cm^{-1}$ and 433.39 $cm^{-1}$, corresponding to Cu–O stretching modes, confirming metal-oxygen bonding. Peaks at 3136.73 $cm^{-1}$ (O–H stretching) and 1654.94 $cm^{-1}$ (C=O stretching) suggested the presence of organic residues. The nanoscaffolds showed signature peaks at 3297.44 $cm^{-1}$ (O–H stretch), 1424.21 $cm^{-1}$ (C–H bending), and 1108.87 $cm^{-1}$ (C–O–C stretching), consistent with polysaccharide and PVA components. Additional bands below 1000 $cm^{-1}$ (940.79 $cm^{-1}$ and 601.52 $cm^{-1}$) indicated polymer-metal interactions, confirming successful CuO NP incorporation within the scaffold matrix.

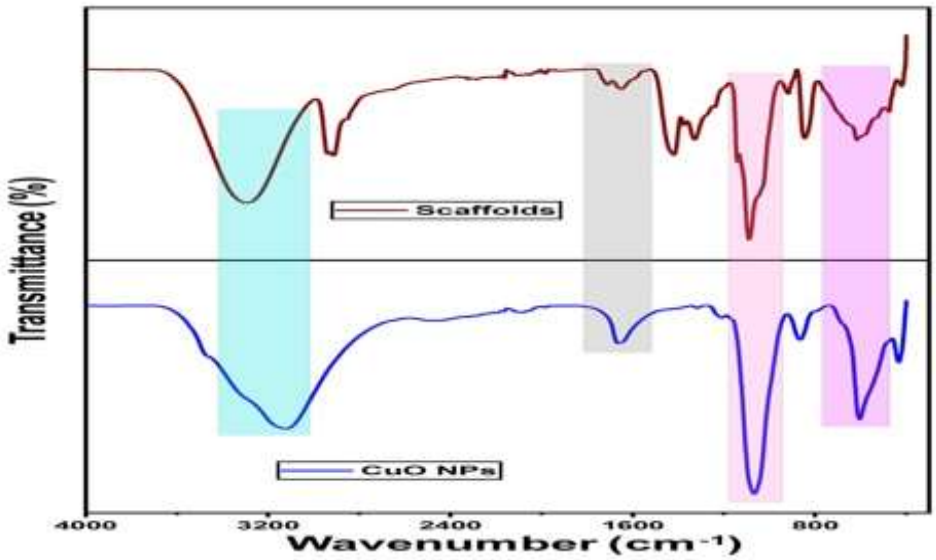


**Fig. 2. FTIR spectra of CuO NPs and their incorporation into nanoscaffolds.**

### 3.3. XRD analysis

XRD patterns (Fig. 3) recorded using a Bruker D8 Advance diffractometer with CuKα radiation (λ = 1.5406 Å) validated the crystalline nature of both CuO NPs and starch/PVA nanoscaffolds. The CuO NPs displayed sharp diffraction peaks between 2θ angles of 13.310° and 56.302°, corresponding to the monoclinic tenorite phase (JCPDS no. 05-0661). The most intense peak at 18.938° (d-spacing: 4.68228 Å) reflected pronounced crystallinity. Conversely, nanoscaffolds exhibited a semi-crystalline structure, with prominent peaks at 21.307° (d = 4.16681 Å) and 29.349° (d = 3.04070 Å), accompanied by broad amorphous regions. The scaffold's pattern indicated an amorphous content of 82.9% and a crystalline fraction of 17.1%. The absence of extraneous peaks confirmed the purity and composite integrity of the material.

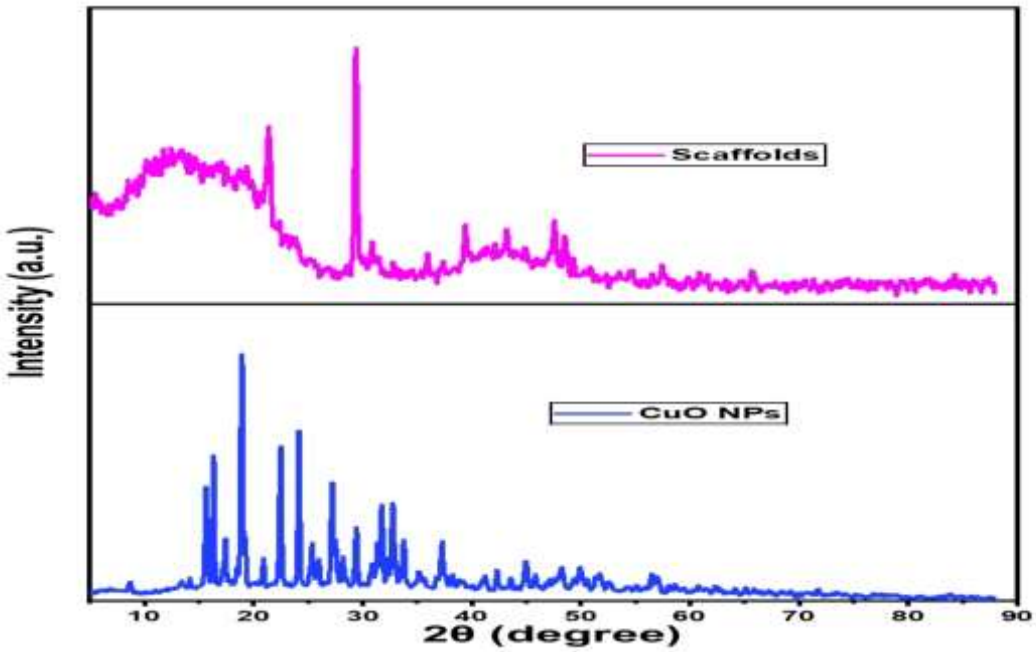


**Fig. 3. XRD patterns of synthesized CuO NPs and CuO-loaded scaffolds.**

### 3.4. SEM analysis

Surface morphology was examined through SEM using a JEOL JSM-IT800 NANO instrument. The CuO NPs appeared as homogeneously dispersed particles, exhibiting shapes ranging from spherical to irregular (Fig. 4). The starch/PVA nanoscaffolds revealed a porous, interconnected fibrous network characterized by smooth, continuous, and bead-free fibers. CuO NPs were uniformly embedded within the polymeric framework without visible aggregation. The scaffold's three-dimensional porous morphology supports its suitability for biomedical applications by facilitating nutrient diffusion and cell infiltration. These structural characteristics confirm effective electrospinning and nanoparticle incorporation.

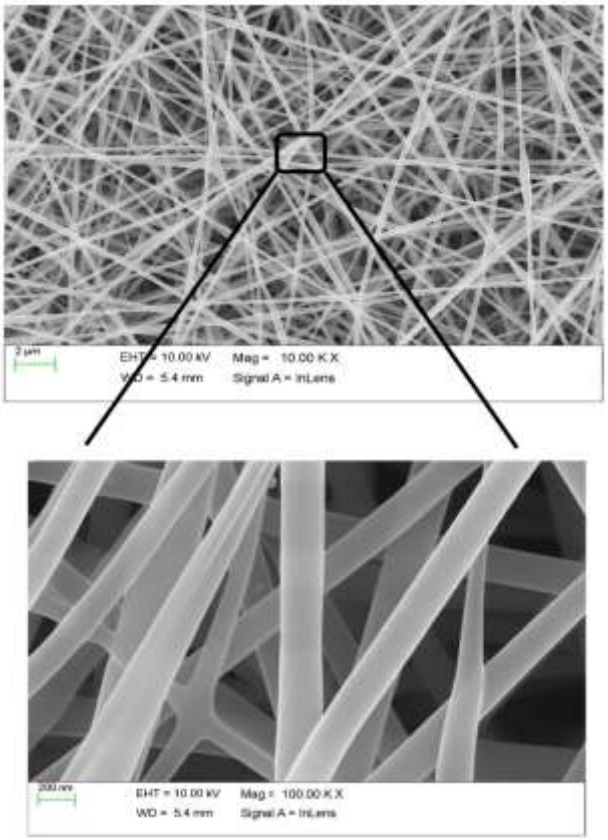


**Fig. 4. SEM analysis of synthesized CuO NPs and CuO-loaded scaffolds.**

### 3.5. TGA

Thermal behavior of the starch/PVA nanoscaffolds (Fig. 5) was evaluated via TGA using a PerkinElmer instrument under nitrogen flow, with heating from 30°C to 550°C at 15°C/min. Initial mass loss below 150°C was attributed to moisture evaporation. Major thermal degradation commenced at 298.21°C, peaked at 356.55°C, and concluded by 395.85°C, corresponding to polymeric matrix breakdown. The total mass loss reached 41.912%, indicating significant organic decomposition. The nanoscaffolds demonstrated thermal stability up to approximately 300°C, followed by rapid decomposition. These results align with typical thermal profiles for biopolymer-based materials and help define thermal limits for biomedical usage.

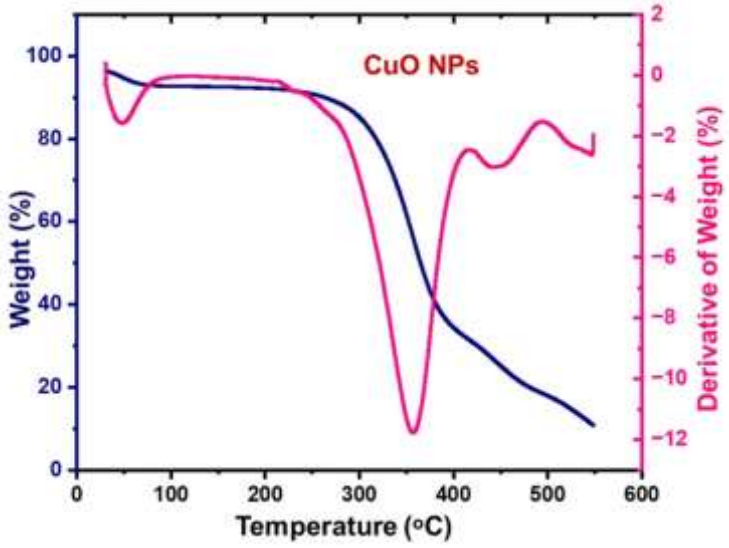


**Fig. 5. Thermal degradation behavior of CuO-incorporated nanoscaffolds.**

### 3.6. Zeta potential and particle size analysis

DLS analysis using a Malvern Zetasizer showed that CuO NPs had a hydrodynamic diameter (Z-average) of 108 nm (Fig. 6). Zeta potential measurements revealed an average surface charge of -22.13 mV, with distinct subpopulations at -30.51 mV and -16.71 mV (Fig. 7), indicative of moderate colloidal stability. The negative surface charge arises from functional groups on the particle surface, although the zeta potential values below ±30

mV suggest a tendency toward aggregation. The sample exhibited a conductivity of 0.03211 mS/cm and derived count rates of 1570 kcps. These findings provide important insights into the dispersion stability and potential biocompatibility of the nanoparticles.

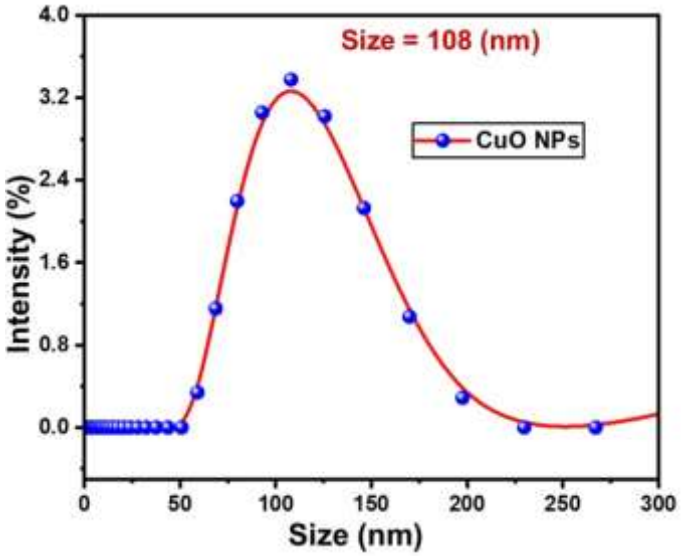


**Fig.6. DLS particles size analysis of CuO NPs**

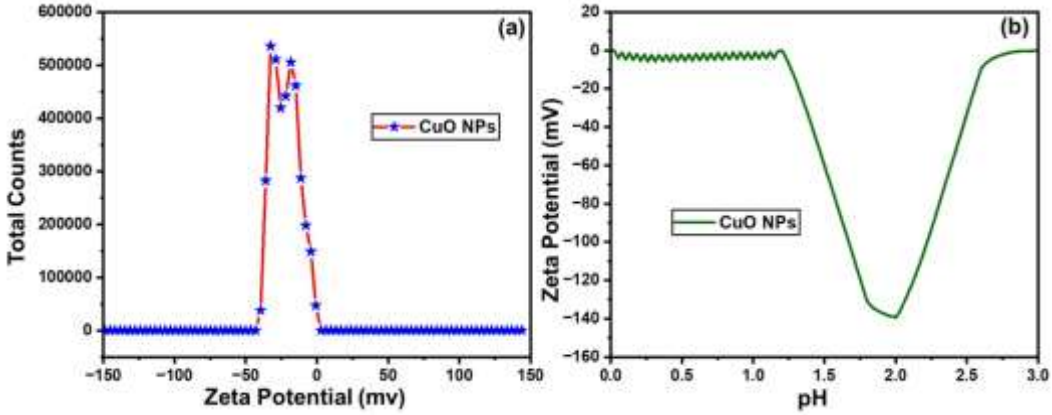


**Fig.7. Zeta-potential analysis of CuO NPs**

### 3.7. *In vitro* anticancer activity

The *in vitro* anticancer activity of algal extract, copper CuO NPs, and starch/PVA/CuO-NPs nanoscaffolds was evaluated against HT-29 colon cancer cells and MCF-7 breast cancer cells using the MTT assay (Fig. 8). The results demonstrated concentration-dependent cytotoxicity for all tested compounds, with varying degrees of potency observed across the different formulations.

Against HT-29 cells, the algal extract exhibited moderate anticancer activity, reducing cell viability from 97.7% at the lowest concentration (6.25 µg/mL) to 36.45% at the highest concentration (100 µg/mL). The $IC_{50}$ value, representing the concentration required to inhibit 50% of cell growth, was estimated to be approximately 30–35 µg/mL. In comparison, CuO NPs showed stronger cytotoxic effects, decreasing viability from 82.7% to 26.03% over the same concentration range, with an $IC_{50}$ of around 15–20 µg/mL. The starch/PVA/CuO-NPs nanoscaffolds demonstrated the highest efficacy, causing a sharp decline in viability from 79.1% to 19.08%, and achieving an $IC_{50}$ of approximately 10–12 µg/mL.

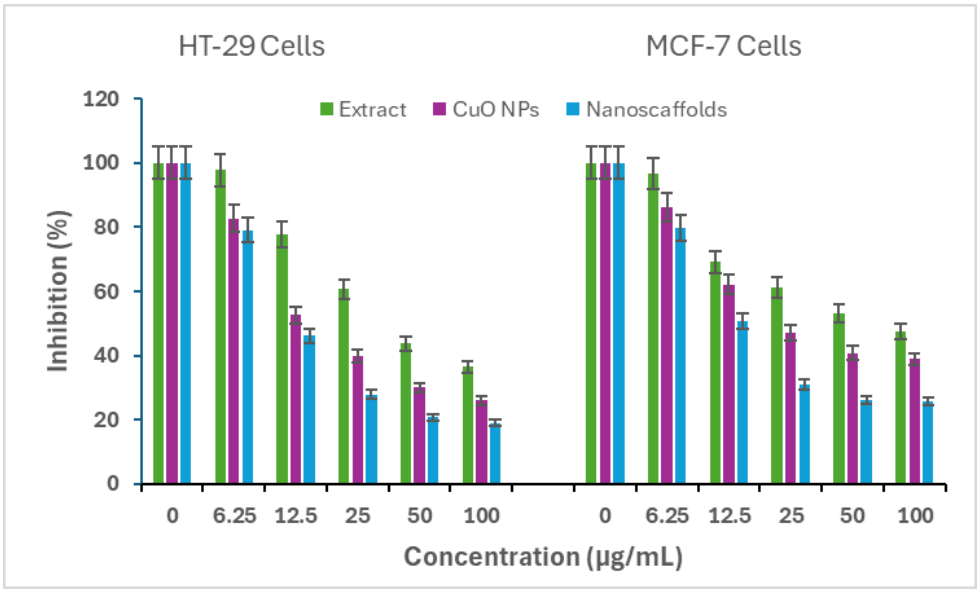


**Fig. 8. Anticancer activity analysis of algal extract, CuO-NPs and starch/PVA/CuO-NPs nanoscaffolds**

Similar trends were observed in MCF-7 cells, though the overall sensitivity to the compounds was slightly lower. The algal extract reduced viability from 96.7% to 47.45%, yielding an $IC_{50}$ of about 40–45 µg/mL. CuO NPs exhibited improved activity, lowering viability from 86.2% to 38.87%, with an $IC_{50}$ of 20–25 µg/mL. Once again, the nanoscaffolds outperformed the other formulations, decreasing viability from 79.8% to 25.82% and achieving an $IC_{50}$ of 12–15 µg/mL.

These findings highlight the superior anticancer potential of starch/PVA/CuO-NPs nanoscaffolds, which exhibited the lowest $IC_{50}$ values against both cancer cell lines. CuO NPs demonstrated intermediate activity, while the algal extract showed the least cytotoxicity. The results suggest that the nanoscaffold formulation enhances the delivery or potency of the active components, making it a promising candidate for further development in cancer therapy. The study underscores the importance of nanomaterial-based approaches in improving the efficacy of anticancer agents.

## 4. DISCUSSION

The UV-Visible spectral analysis clearly substantiates the successful synthesis of CuO NPs using the *P. tetrastromatica* extract. The distinct absorption peak observed at 273 nm is indicative of surface plasmon resonance (SPR), a phenomenon commonly associated with metal and metal oxide nanoparticles due to collective oscillations of conduction electrons on the nanoparticle surface. This peak confirms the formation of nanoscale CuO particles, consistent with prior literature reporting characteristic SPR peaks in similar wavelength regions for copper oxide nanostructures. In contrast, the absence of a defined peak in the algal extract suggests the lack of nanoparticle formation in the raw biological material, emphasizing the distinct optical signatures of nanoparticles versus bulk biological compounds. The precise wavelength range and scan parameters further reinforce the reliability of these observations, underscoring UV-Vis spectroscopy as a rapid, non-destructive tool for monitoring nanoparticle synthesis and differentiation from precursor extracts [42-47].

FTIR spectroscopy provided detailed insights into the chemical environment and bonding within both the synthesized CuO NPs and the composite starch/PVA nanoscaffolds. The signature absorption bands in the low wavenumber region at approximately 603 $cm^{-1}$ and 433 $cm^{-1}$ strongly correspond to Cu–O stretching vibrations, unequivocally confirming the metal-oxygen bonding crucial to CuO's structural integrity. Meanwhile, the presence of broad hydroxyl (O–H) and carbonyl (C=O) peaks hints at residual organic moieties, likely originating from biomolecules within the algal extract that act as reducing and capping agents during nanoparticle formation. In the composite scaffolds, the characteristic peaks for polysaccharide and PVA components confirm the successful blending of these biopolymers. Importantly, the appearance of bands below 1000 $cm^{-1}$ associated with metal-polymer interactions indicates effective incorporation and binding of CuO NPs within the polymeric matrix. This integration is vital for ensuring uniform dispersion, enhancing the mechanical and functional properties of the scaffold, and preventing nanoparticle aggregation [48-53].

XRD analysis further confirmed the crystalline nature of the CuO NPs, with the observed peaks matching the monoclinic tenorite phase, a well-known crystalline form of CuO. The sharp, intense peaks reflect high crystallinity, essential for consistent physicochemical properties and bioactivity. The starch/PVA nanoscaffolds exhibited a semi-crystalline structure with predominant amorphous regions, typical for biopolymer blends. The amorphous content exceeding 80% suggests flexibility and porosity, beneficial for biomedical scaffolds as it can support cell adhesion and nutrient diffusion. Additionally, the absence of extraneous diffraction peaks indicates the purity and phase stability of both the nanoparticles and the composite scaffold. These structural insights

confirm that the electrospinning process preserved the crystallinity of CuO while achieving a composite scaffold with the desired amorphous-crystalline balance [54-59].

SEM offered a direct visualization of the surface morphology and confirmed the nanoscale size and distribution of the CuO particles. The homogeneous dispersion of nanoparticles ranging from spherical to irregular shapes within the polymeric network highlights successful nanoparticle incorporation without agglomeration, which is crucial for maintaining consistent biological activity and mechanical integrity. The porous, interconnected fibrous architecture of the starch/PVA scaffold mimics the extracellular matrix, facilitating cellular infiltration and nutrient transport—key parameters for tissue engineering and drug delivery applications. The smooth, bead-free nature of the fibers attests to the optimized electrospinning conditions, which produced uniform fibers capable of supporting the structural and functional demands of biomedical scaffolds [60-66].

TGA demonstrated the thermal stability of the starch/PVA/CuO nanoscaffolds, revealing an initial moisture loss phase followed by a major decomposition event linked to the polymer matrix degradation. The onset of degradation near 300°C aligns with typical thermal behavior of starch and PVA composites, confirming the scaffold's suitability for biomedical applications requiring sterilization or moderate thermal processing. The considerable organic mass loss also reflects the composite's biopolymeric composition, ensuring biodegradability, which is advantageous for temporary implants or controlled release systems. These thermal profiles help delineate operational temperature ranges, ensuring the scaffold's structural integrity is maintained during storage and use [67-71].

DLS and zeta potential measurements provided critical information on nanoparticle size distribution and surface charge, parameters that influence colloidal stability and biological interactions. The average hydrodynamic size of approximately 108 nm falls within the optimal range for cellular uptake and enhanced permeability in cancer therapy. The negative surface charge observed, while moderate, suggests some degree of colloidal stability due to electrostatic repulsion; however, zeta potential values below ±30 mV hint at a potential for particle aggregation over time, which might be mitigated by surface functionalization or stabilization strategies. The conductivity and derived count rate values support stable dispersion in aqueous media, an important aspect for biological applications [72-74].

Most notably, the *in vitro* anticancer activity assays reveal a clear enhancement of cytotoxic effects when CuO NPs are integrated into starch/PVA nanoscaffolds. The scaffold formulation exhibited the lowest $IC_{50}$ values against both HT-29 colon and MCF-7 breast cancer cells, outperforming both the algal extract alone and CuO NPs in suspension. This increased potency likely arises from improved bioavailability, sustained release, and enhanced cellular uptake afforded by the nanofibrous scaffold matrix. The concentration-dependent cytotoxicity confirms the therapeutic potential, with the scaffold likely facilitating better interaction between the nanoparticles and cancer cells. The differential sensitivities between the two cancer cell lines also underscore the importance of targeted delivery systems, as cell-specific uptake and response can vary. Collectively, these findings highlight the promise of combining natural extracts with nanotechnology to develop advanced cancer therapeutics, emphasizing the role of biopolymer-based scaffolds as effective delivery platforms that can enhance the efficacy of nanoparticulate agents [75-78].

## 5. CONCLUSION

This study successfully demonstrated the green synthesis of copper oxide nanoparticles using *P. tetrastromatica* extract, confirmed through UV-Vis, FTIR, XRD, and SEM analyses. The integration of CuO NPs into starch/PVA nanoscaffolds was achieved effectively, as evidenced by structural and chemical characterizations indicating strong polymer–nanoparticle interactions and maintained crystallinity. The fabricated nanoscaffolds exhibited favorable thermal stability and a porous, fibrous architecture suitable for biomedical applications. DLS and zeta potential analyses revealed nanoparticles with optimal size and moderate colloidal stability, essential for therapeutic delivery. Importantly, the *in vitro* anticancer assays against HT-29 and MCF-7 cell lines established that the starch/PVA/CuO nanoscaffolds significantly enhanced cytotoxic effects compared to the algal extract and CuO nanoparticles alone, indicating improved bioavailability and efficacy. These findings underscore the potential of biopolymer-based nanocomposites as promising candidates for cancer therapy, combining natural extracts with nanotechnology to achieve controlled delivery and enhanced therapeutic performance.

**Ethics declaration:** Not Applicable

**Funding Declaration:** No funding available for this study.

**Data Availability Statement:** The full dataset of physiochemical characterization associated with this work is published in Mendeley Data [Dataset] Padina tetrastromatica-driven synthesis meets biopolymers: comprehensive profiling of starch nanoscaffolds infused with eco-friendly copper oxide nanoparticles (DOI: 10.17632/ddbgcpm32x.1). Disclosure: The material characterization data and figures (e.g., UV, SEM, FTIR, XRD, TGA, Zeta Potential and particle sizer) presented here were generated from a common dataset and are being reused across multiple related studies on nanomaterials. All biological analyses and conclusions are original to each manuscript.

**Conflicts of Interest:** The authors declare no conflicts of interest.

**REFERENCES**


[1] Kunamalla RP, Panagal M, Palanisamy CP. Green-engineered multiscale starch/PVA nanofibrous scaffolds embedded with CuO nanoparticles from Sargassum ilicifolium for potent antimicrobial performance. Genetics and Molecular Research. 2026; 25(13s): 1-9.

[2] Dharmaprakash S, Gunasekaran VP, Sivaramakrishnan R, Kanniappan GV, Jayaraman S, Mironescu M, Rajabathar JR, Mironescu ID, Palanisamy CP. Marine macroalgae-mediated ultrasonic-assisted green synthesis of CuO nanoparticles embedded in starch/PVA electrospun nanoscaffolds for in vitro α-amylase and α-glucosidase inhibitory activity. Scientific Reports. 2026; 16: 26243.

[3] Surendran N, Chandrasekaran G, Raju MV, Chandrasekaran MK, Ahalliya RM, Palanisamy CP, Kanniappan GV, Arcot R, Alharbi NS, Thiruvengadam M. Anti-inflammatory potential of ethanolic extract of Maranta arundinacea L.: Insights from COX-2 modulation and oxidative stress analysis. South African Journal of Botany. 2026; 195: 142-151.

[4] Pei J, Senthilkumar MV, Hessini K, Subramaniyam S, Sivaramakrishnan R, Kanniappan GV, Jayaraman S, Palanisamy CP. Green fabrication of starch/PVA/CuO nanoscaffolds using marine macroalgae extract for enhanced anti-inflammatory activity. Sustainable Chemistry and Pharmacy. 2026; 51: 102397.

[5] Balasubramanian V, Loganathan L, Muthuswamy K, Viswanathan TM, Raju MV, Chandrasekaran MK, Ahalliya RM, Poorasamy J, Palanisamy CP, Dominic S, Kanniappan GV. Anticancer therapeutic efficacy of PEGylated β-galactosidase from Aspergillus terreus in DMBA-induced breast cancer: Toxicological, molecular and histopathological evaluation in Wistar rats. International Journal of Biological Macromolecules. 2026; 360: 151856.

[6] Jayaraman S, Eswaran A, Rajagopal P, Palanisamy CP, Veerakumar P, Veeraraghavan VP, Sirasanagandla SR. Neuroendocrine-associated epigenetic factors in cellular senescence: mechanisms and therapeutic implications. Biogerontology. 2026; 27(2): 64.

[7] Ponnusamy B, Rajagopal P, Palanisamy CP, Veeraraghavan VP, Jayaraman S. Mechanistic Exploration of the anticancer activity of Justicia adhatoda Plant Leaf Ethanolic Extract against Colon Cancer Cells: An in silico and in vitro Approach. Asian Pacific Journal of Cancer Prevention. 2026; 27(3): 1069-1080.

[8] Pei J, Saran VS, Sivaramakrishnan R, Kanniappan GV, Pandurangan V, Jayaraman S, Dhayalan VK, Mironescu M, Mironescu ID, Palanisamy CP. Ultrasonic-assisted, Sargassum ilicifolium (brown marine macroalgae)-mediated biogenic synthesis of CuO nanoparticles incorporated in starch/PVA electrospun nanoscaffolds: In vitro safety and antioxidant efficacy assessment. Bioorganic Chemistry. 2026; 173: 109679.

[9] Raj MAPA, Subramaniyam S, Kanniappan GV, Jayaraman S, Palanisamy CP. Sustainable fabrication of starch/PVA/CuO electrospun nanoscaffolds from Turbinaria ornata (marine macroalgae) extract: Physicochemical characterization and antidiabetic evaluation. Kuwait Journal of Science. 2026; 53(2): 100545.

[10] Pei J, Ganesh NS, Subramaniyam S, Sivaramakrishnan R, Kanniappan GV, Jayaraman S, Palanisamy CP. Sustainable fabrication of starch/PVA/CuO electrospun nanoscaffolds from Padina tetrastromatica (Brown macroalgae) extract: Physicochemical characterization and antidiabetic assessment. Sustainable Chemistry One World. 2026; 9: 100195.

[11] Sakthiraj A, Sivaramakrishnan R, Subramaniyam S, Kanniappan GV, Pandurangan V, Jayaraman S, Dhayalan VK, Mironescu M, Mironescu ID, Palanisamy CP. Starch/PVA electrospun nanoscaffolds loaded with ultrasonic-assisted green-synthesis of CuO nanoparticles from marine macroalgae (Gracilaria corticata) extract: Cytotoxicity and antioxidant analysis. Chemical Physics Impact. 2026; 12: 101018.

[12] Raju M, Chandrasekaran MK, Loganathan L, Ahalliya RM, Mironescu M, Mironescu ID, Palanisamy CP, Kanniappan GV. Lipid remodeling and ferroptosis in phosphatidylcholine-mediated tumor–stroma crosstalk. Frontiers in Molecular Biosciences. 2026; 13: 1742305.

[13] Kunamalla R, Panagal M, Palanisamy CP. Biogenic synthesis and fabrication of starch/PVA/CuO electrospun nanoscaffolds from Sargassum ilicifolium (brown marine macroalgae) extract for anticancer activity on HT-29 and MCF-7 cancer cells. Biocatalysis and Agricultural Biotechnology. 2026; 72: 103923.

[14] Pei J, Govindaraj H, Sivaramakrishnan R, Kanniappan GV, Pandurangan V, Dhayalan VK, Mironescu M, Mironescu ID, Jayaraman S, Palanisamy PC. Sustainable fabrication of biopolymer-based (starch/PVA) nanoscaffolds loaded with green-synthesized CuO nanoparticles from Sargassum wightii (marine macroalgae): Cytocompatibility and antioxidant activity. Biomaterials Advances. 2026; 182: 214660.

[15] Pei J, Perumal NC, Meng P, Long Q, Palanisamy CP. Extracellular vesicle-based biosensors for Alzheimer's disease: A new frontier in precision diagnostics. Ageing Research Reviews. 2026; 113: 102904.

[16] Shree P, Sivaramakrishnan R, Kanniappan GV, Pandurangan V, Jayaraman S, Dhayalan VK, Mironescu M, Mironescu ID, Palanisamy CP. Antioxidant and biocompatible CuO-starch/PVA nanoscaffolds via ultrasonic green synthesis using Turbinaria conoides (brown marine macroalgae). Medicine in Drug Discovery. 2025; 28: 100238.

[17] Gong J, Lin J, Guan T, Pei J, Palanisamy CP, El-AtyFrom AMA. selenium tolerance to nanoplastic antagonism: Comprehensive characterization of L. casei SNUT1 and its extracellular vesicle–nanoselenium complex. Food Bioscience. 2025; 74: 107749.

[18] Poochi SP, Sundarraj R, Raju MV, Chandrasekaran MK, Ahalliya RM, Palanisamy CP, Kanniappan GV,

Kondapavuluri BK, Thiruvengadam M. Harnessing Nature: Computational and Experimental Insights Into *Ipomoea obscura* Metabolites for Bladder Cancer Therapy. Chemistry and Biodiversity. 2025; 0: e00909.
[19] Dugganaboyana GK, Kannankumar MKG, Shivaramakrishna S, Raju MV, Chandrasekaran MK, Ahalliya RM, Panneerselvam N, Palanisamy CP, Kanniappan GV. Phytochemical insights, antioxidant activity and therapeutic potential of Cassia senna against prostate cancer in Wistar albino rats. Discover Applied Sciences. 2025; 7:1206.
[20] Natarajan SR, Krishnamoorthy R, Alshuniaber MA, Gatasheh MK, Rajagopal P, Veeraraghavan VP, Palanisamy CP, Jayaraman S. KDM1A Facilitates Oncogenic Potential in Colorectal Cancer Progression Through the Activation of AXIN/GSK3β/β-Catenin Signaling Pathways: Evidence From Integrated Transcriptomics and In Vitro Studies. The Journal of Gene Medicine. 2025; 27(11): e70053.
[21] Guan T, Gong J, Lin J, Palanisamy CP, Jinjin Pei J, El-Aty AMA. Machine learning-driven multimodal optimization of selenium biotransformation and flavor profiling in fermented apple–Yacon functional beverages. Innovative Food Science & Emerging Technologies. 2025; 105: 104198.
[22] Natarajan SR, Krishnamoorthy R, Alshuniaber MA, Alsulami TS, Gatasheh MK, Rajagopal P, Palanisamy CP, Govindan R, Veeraraghavan VP, Jayaraman S. ABCE1 facilitates tumour progression via aerobic glycolysis and inhibits cell death in human colorectal cancer cells through the p53 signalling pathway. Scientific Reports. 2025; 15: 24674.
[23] Huang Y, Guo H, Liu Y, Jin W, Palanisamy CP, Pei J, Oz F, El-Aty AMA. Effects of Natural Polysaccharides on the Gut Microbiota Related to Human Metabolic Health. Molecular Nutrition & Food Research. 2025; 69:e202400792.
[24] Poornima K, Meenakshi K.C, Manikandan V.R, Shankari G, Prabhu D, Rathi M.A, Palanisamy CP, Balaji R, Gopalakrishnan V.K. Exploring the anticancer potential of Jerantinine A from *Tabernaemontana coronaria* against prostate, breast, and ovarian cancers: A computational approach. *Journal of Complementary and Integrative Medicine*, 2025 22(2): 363–372.
[25] Palanisamy CP, Poompradub S, Sansanaphongpricha K, Jayaraman S, Subramani K. Faridah Sonsudin gGreen synthesis of Nigella sativa-mediated silver nanoparticles for enhanced antibacterial activity and wound healing: Mechanistic insights and biomedical applications. Environmental Nanotechnology, Monitoring & Management. 2025; 24: 101085.
[26] Surendran N, Raju MV, Chandrasekaran MK, Ahalliya RM, Palanisamy CP, Chandrasekaran G, Kanniappan GV. Physicochemical characterization of starch from Maranta arundinacea L.(arrowroot) rhizomes and its inhibition of COX-2: In vivo validation. Bioactive Carbohydrates and Dietary Fibre. 2025; 33: 100465.
[27] Pei JJ, Perumal NC, Meng P, Long Q, Palanisamy CP. AI-assisted FTIR spectroscopic profiling of exosomes: Emerging frontiers in early detection of Alzheimer's disease. Ageing Research Reviews. 2026; 103311.
[28] Raja FSD, Abraham L, Rangasamy K, Saikia K, Rathankumar AK, Mironescu M, Mironescu I, Palanisamy CP, Kanniappan GV. Next-Generation Microbiome Therapeutics: Psychobiotics and Fecal Microbiota Transplants (FMT) for Mental Health Treatment. Frontiers in Cellular and Infection Microbiology. 2026; 16: 1719357.
[29] Subramani K, Srinivasan S, Shanmugam P, Palanisamy CP, Sonsudin F, Poompradub S. Sustainable phytochemical mediated-ZnO nanoparticles derived from Crescentia cujete for toxicological evaluation and multifunctional environmental applications. Environmental Nanotechnology, Monitoring & Management. 2026; 26: 101180.
[30] Natarajan PM, Umapathy VR, Murali A, Swamikannu B. (2022). Computational Simulations of Identified marine-derived Natural Bioactive Compounds As Potential Inhibitors of Oral Cancer. Future Science OA. 2022; 8(3).
[31] Natarajan PM, Umapathy VR. Role of transcriptomics in the study of oral cancer. Frontiers in Oral Health. 2025; 6:1524364.
[32] Vidhyarekha U, Natarajan PM, Bhuminathan S, Sabarinathan J, Suba R, Vijayalakshmi P. Role of artificial intelligence in Oral Cancer. Advances in Public Health. 2024. 2024: 3664408.
[33] Ganesan A, Kumar NG, Natarajan PM, Gauthaman J. Automated classification of elongated styloid processes using deep learning models-an artificial intelligence diagnostics. Frontiers in Oral Health. 2025; 5: 1424840.
[34] Umapathy VR, Natarajan PM, Swamikannu B. Regenerative Strategies in Dentistry: Harnessing Stem Cells, Biomaterials and Bioactive Materials for Tissue Repair. Biomolecules. 2025; 15: 546.
[35] Natarajan PM. Dental Bioinformnatics-Current Scope and Future perspectives. Research Journal of Pharmacy and Technology. 2022;15(5):2351-6.
[36] Ganesan A, Kumar NG, Natarajan PM. Solanum trilobatum leaf extract-derived silver nanoparticles downregulate the PI3K/AKT/mTOR signaling pathway and attenuate oral squamous cell carcinoma cell proliferation. Journal of Herbmed Pharmacology. 2024; 13(2): 300-307.
[37] Perumal MKK, Renuka RR, Subbiah SK, Natarajan PM. Artificial intelligence-driven clinical decision support systems for early detection and precision therapy in oral cancer: a mini review. Frontiers in Oral Health. 2025; 6: 1592428.

[38] Ramesh E, Ganesan A, Lakshmi KC, Natarajan PM. Artificial intelligence-based diagnosis of oral leukoplakia using deep convolutional neural networks Xception and MobileNet-v2. Frontiers in Oral Health. 2025; 6: 1414524.
[39] Ganesan A, Kumar NG, Natarajan PM. Anticancer activity of silver nanoparticles synthesized from aqueous leaf extract of Solanum trilobatum (Purple fruit pea eggplant) on human oral cancer cells. Journal of Herbmed Pharmacololgy. 2024; 13(2): 260-268.
[40] Kannappan P, Chandrasekaran MK, Raju MV, Gopalakrishnan S, Dhamodharan P, Ahalliya RM, Palanisamy CP, Raju B, Kanniappan GV. Exploring the anticancer potential of Jerantinine A from Tabernaemontana coronaria against prostate, breast, and ovarian cancers: a computational approach. Journal of Complementary and Integrative Medicine. 2025; 22(02): 363-372.
[41] Pei J, Kumarasamy RV, Jayaraman S, Kanniappan GV, Long Q, Palanisamy CP. Quercetin-functionalized nanomaterials: Innovative therapeutic avenues for Alzheimer's disease management. Ageing Research Reviews. 2025; 104: 102665.
[42] Jayaraman S, Prasad M, Natarajan SR, Krishnamoorthy R, Alshuniaber MA, Gatasheh MK, Veeraraghavan VP, Rajagopal P, Palanisamy CP. Molecular mechanisms underlying the effects of beta-sitosterol on TGF-β1/Nrf2/SIRT1/p53-mediated signaling in the kidney of a high-fat diet and sucrose-induced type-2 diabetic rat. Chemico-Biological Interactions. 2025; 411: 111443.
[43] Huang Y, Guo H, Liu Y, Jin W, Palanisamy CP, Pei J, Oz F, El-Aty AMA. Effects of Natural Polysaccharides on the Gut Microbiota Related to Human Metabolic Health. Molecular Nutrition & Food Research. 2025; e202400792.
[44] Prabhakaran P, Palanisamy CP, Shanmugam A, Damodharan P, Swaminathan H, Devaraj D, Ahalliya RM, Kanniappan GV. Isolation, structural characterization, and molecular docking studies on the bioactive compound from n-Hexane extract of Emilia sonchifolia (L.) DC against the pancreatic cancer target Aurora 2 Kinase. Journal of Complementary and Integrative Medicine. 2024; 22(1): 0290.
[45] Jiang H, Kumarasamy RV, Pei J, Raju K, Kanniappan GV, Palanisamy CP. Integrating engineered nanomaterials with extracellular vesicles: Advancing targeted drug delivery and biomedical applications. Frontiers in Nanotechnology. 2024; 6: 1513683.
[46] Guo H, Liu Y, Wan T, Song D, Palanisamy CP, Geng J, Pei J, Özmen S, El-Aty AMA. Toward personalized cancer management: Role of precision nutrition–diet interventions. Journal of Functional Foods. 2024; 123: 106584.
[47] Natarajan SR, Krishnamoorthy R, Alshuniaber MA, Al-Anazi KM, Farah MA, Rajagopal P, Palanisamy CP, Veeraraghavan VP, Jayaraman S. Identification of FOXM1 as a novel protein biomarker and therapeutic target for colorectal cancer progression: Evidence from immune infiltration and bioinformatic analyses. International Journal of Biological Macromolecules. 282 (Part 4): 137201.
[48] Rajendran MS, Jayaraman S, Khan JM, Jasmine S, Prabhakaran RK, Raju MV, Chandrasekaran MK, Ahalliya RM, Kannappan P, Palanisamy CP, Kanniappan GV. Investigating the colon toxicity and carcinogenic role of monosodium glutamate compared with Dimethylhydrazine in male Wistar rats: Exploring the link to childhood colon cancer risk. Journal of King Saud University - Science. 2024; 36(11): 103507.
[49] Kumarasamy RV, Natarajan P, Umapathy VR, Roy JR, Rab SO, Saeed M, Panagal M, Mironescu M, Srinivasan GP, Palanisamy CP. Clinical Applications and Therapeutic Potentials of Advanced Nanoparticles: A Comprehensive Review on Completed Human Clinical Trials. Frontiers in Nanotechnology. 2024; 6:1479993.
[50] Jin W, Pei JJ, Roy JR, Jayaraman S, Ahalliya RM, Kanniappan GV, Mironescu M, Palanisamy CP. Comprehensive review on single-cell RNA sequencing: A new frontier in Alzheimer's disease research. Ageing Research Reviews. 2024; 274: 102454.
[51] Pei J, Palanisamy CP, Jayaraman S, Natarajan PM, Umapathy VR, Roy JR, Panagal M, Jayaraman S. Curcumin-loaded polymeric nanomaterials as a novel therapeutic strategy for Alzheimer's disease: A comprehensive review. Ageing Research Reviews. 2024; 99: 102393.
[52] Pei J, Palanisamy CP, Jayaraman S, Natarajan PM, Umapathy VR, Roy JR, Thalamati D, Ahalliya RM, Kanniappan GV, Mironescu M. A comprehensive review on starch-based Sustainable Edible Films Loaded with Bioactive Components for Food Packaging. International Journal of Biological macromolecules. 2024; 274 (Part-1): 133332.
[53] Palanisamy CP, poompradub S, Sansanaphongpricha K, Subramani K, Sonsudin F. Increased expression levels of PDGF and VEGF magnify the wound healing potential facilitated by biogenic synthesis of silver nanoparticles. Nano-Structures & Nano-Objects. 2024; 39: 101236.
[54] Pei J, Palanisamy CP, Jayaraman S, Natarajan PM, Umapathy VR, Roy JR, Thalamati D, Ahalliya RM, Kanniappan GV, Mironescu M. Proteomics Profiling of Extracellular Vesicle for Identification of Potential Biomarkers in Alzheimer's Disease: A Comprehensive Review. Ageing Research Reviews. 2024; 99: 102359.
[55] Xi J, Wang T, Xian P, Liu X, Du M, Yang H, Palanisamy CP, Lin W, Long Q. Proteomic insights uncover enhanced neurotherapeutic potential in conditioned mesenchymal stem cell-derived extracellular vesicles. Extracellular Vesicle. 2024; 3: 100037.
[56] Pei J, Natarajan PM, Umapathy VR, Swamikannu B, Sivaraman NM, Krishnasamy L, Palanisamy CP. Advancements in the synthesis and functionalization of zinc oxide-based nanomaterials for enhanced oral cancer therapy. Molecules. 2024; 29(11): 2706.

[57] Gatasheh MK, Natarajan SR, Krishnamoorthy R, Alsulami TS, Rajagopal P, Palanisamy CP, Veeraraghavan VP, Jayaraman S. Molecular analysis to identify novel potential biomarkers as drug targets in colorectal cancer therapy: an integrated bioinformatics analysis. Molecular and Cellular Oncology. 2024; 11(1): 2326699.
[58] Natarajan PM, Swamikannu B, Sivaraman NM, Stylin AGSQ. Prevention of Oral Cancer: A Comprehensive Guide. Journal of Pharmacy and Bioallied Sciences. 2024; 16(5): S4239-S4241.
[59] Umapathy V, Dhanavel A, Kesavan R, Natarajan PM, Bhuminathan S, Vijayalakshmi P. Anticancer Potential of the Principal Constituent of Piper nigrum, Piperine: A Comprehensive Review. Cureus. 2024; 16(2): e54425.
[60] Umapathy VR, Swamikannu B, Natarajan PM, Devi R, Nandini MS, Vimalarani, Vijayalakshmi P. In Silico Molecular Docking of Ocimum sanctum Phytochemicals: Targeting Key Biomarkers in Oral Cancer. Journal of Pharmacy and Bioallied Sciences. 2024; 16(5): S4792-S4799.
[61] Natarajan PM, Bhuminathan S, Rajan R, Bindu K, Loganathan K, Veerakumar R. The Crucial Role of Smoking Cessation in Preventing Oral Cancer. Journal of Pharmacy and Bioallied Sciences. 2024; 16(5): S4245-S4247.
[62] Swamikannu B, Umapathy VR, Natarajan PM, Nandini MS, Stylin AGSQ, Vimalarani V, Rajinikanth S. Unlocking the Therapeutic Benefits of Artemisia Annua: A Comprehensive Overview of its Medicinal Properties. Journal of Pharmacy and Bioallied Sciences. 2024; 16(5): S4248-S4253.
[63] Natarajan PM. Computational Studies on Recent Congeners of Fluoroquinolones and Nitroimidazoles for Their Use in Periodontal Therapy. Journal of Pharmacy and Bioallied Sciences. 2024; 16(5): S4731-S4740.
[64] Yadalam PK, Arumuganainar D, Natarajan PM, Ardila CM. Artificial intelligence-powered prediction of AIM-2 inflammasome sequences using transformers and graph attention networks in periodontal inflammation. Scientific Reports. 2025; 15: 8733.
[65] Yadalam PK, Chatterjee S, Natarajan PM, Ardila CM. Comparison of light gradient boosting and logistic r egression for interactomic hub genes in Porphyromonas gingivalis and Fusobacterium nucleatum-induced perio dontitis with Alzheimer's disease. Frontiers in Oral Health. 2025; 6:1463458.
[66] Natarajan PM, Bhuminathan S, Leela B, Bindu K, Loganathan K, Ramachandran V. Smoking and its Role in Oral Cancer. Journal of Pharmacy and Bioallied Sciences 16(5): S4242-S4244.
[67] Yadalam PK, Natarajan PM, Ardila CM. Variational graph autoencoder for reconstructed transcriptomic data associated with NLRP3 mediated pyroptosis in periodontitis. Scientific Reports. 2025; 15: 1962.
[68] Pei J, Yan Y, Jayaraman S, Rajagopal P, Natarajan PM, Umapathy VR, Gopathy S, Roy JR, Sadagopan CS, Thalamati D, Palanisamy CP, Mironescu M. A review on advancements in the application of starch-based nanomaterials in biomedicine: Precision drug delivery and cancer therapy. International Journal of Biological Macromolecules. 2024; 130746.
[69] Pei JJ, Yan Y, Palanisamy CP, Jayaraman S, Natarajan PM, Umapathy VR, Gopathy S, Roy JR, Sadagopan JC, Thalamati D, Mironescu M. Materials-based drug delivery approaches: Recent advances and future perspectives. Green Processing and Synthesis. 2024; 13: 20230094.
[70] Pei JJ, Deng W, Liu Y, Guo Y, Chen J, Abdu H, Khan MR, Palanisamy CP, El-Aty AM. A Comprehensive Review of Cornus officinalis: Health Benefits, Phytochemistry, and Pharmacological Effects for Functional Drug and Food Development. Frontiers in Nutrition. 2023; 10: 1309963.
[71] Alugoju P, Palanisamy CP, Anthikapalli NVA, Jayaraman S, Prasanskulab A, Chuchawankul S, Dyavaiah M, Tencomnao T. Exploring the anti-aging potential of natural products and plant extracts in budding yeast Saccharomyces cerevisiae: A review. F1000Research. 2023; 12: 1265.
[72] Lavanya M, Krishnamoorthy R, Alshuniaber MA, Manoharadas S, Palanisamy CP, Veeraraghavan VP, Jayaraman S, Rajagopal P, Padmini R. Formulation, characterization and evaluation of gelatin-syringic acid/zinc oxide nanocomposite for its effective anticancer, antioxidant and anti-inflammatory activities. Journal of King Saud University-Science. 2023; 35: 102909.
[73] Palanisamy CP, Poompradub S, Sansanaphongpricha K, Jayaraman S, Subramani K, Sonsudin F. Biosynthesis of silver nanoparticles (AgNPs) using ethanolic extract of Nigella sativa (L.) seeds promotes wound healing via PDGF and VEGF signalling pathways activation. Biocatalysis and Agricultural Biotechnology. 2023; 54: 102970.
[74] Prasad M, Jayaraman S, Natarajan SR, Veeraraghavan VP, Krishnamoorthy R, Gatasheh MK, Palanisamy CP, Elrobh M. Piperine modulates IR/Akt/GLUT4 pathways to mitigate insulin resistance: Evidence from animal and computational studies. International Journal of Biological Macromolecules. 2023; 253: 127242.
[75] Palanisamy CP, Pei JJ, Phaniendra A, Venkata AAN, Jayaraman S, Veeraragahavan VP, Sridevi G, Roy JR, Janaki CS, Thalamati D, Mironescu M, Luo Q, Chai Y, Long Q. New Strategy of Neurodegenerative Disease Treatment with Extracellular Vesicles (EVs) Derived from Mesenchymal Stem Cells (MSCs). *Theranostics*. 2023; 13(12):4138-4165. doi:10.7150/thno.83066.
[76] Palanisamy CP, Phaniendra A, Jayaraman S, Poompradub S. *Nigella sativa* L. seed extracts promotes wound healing progress by activating VEGF and PDGF signalling pathways: *An in vitro* and *in silico* study. *F1000 Research*. 2023; 12: 436.
[77] Pei JJ, Palanisamy CP, Phaniendra A, Venkata AAN, Natarajan PM, Umapathy VR, Swamikannu B, Jayaraman S, Rajagopal P, Poompradub S. A comprehensive review on bio-based materials for chronic diabetic wounds. *Molecules*. 2022; 28(2), 604.